PHYSICAL REVIEW D

PARTICLES AND FIELDS

THIRD SERIES, VOLUME 40, NUMBER 4 15 AUGUST 1989

Matter-enhanced neutrino oscillations in the standard solar model

J. N. Bahcall
Institute for Advanced Study, Princeton, New Jersey 08540

W. C. Haxton
Institute for Nuclear Theory, Department of Physics, FM-15, University of Washington, Seattle, Washington 98195
(Received 10 April 1989)

The effects of matter-enhanced neutrino oscillations on solar-neutrino experiments can be calculated accurately only if uncertainties in the standard solar model are treated properly. As the oscillation probability depends on the neutrino energy, while modifications in the parameters of the standard solar model produce correlated changes in the various solar-neutrino sources, Monte Carlo calculations appear to offer the only means for addressing this problem. We consider the effects of matter-enhanced neutrino oscillations for 1000 standard solar models that were constructed by varying the solar input parameters according to their estimated probability distributions. From these Monte Carlo calculations [carried out for a neutrino parameter grid of 10^4 cases corresponding to 3×10^8 separate Mikheyev-Smirnov-Wolfenstein (MSW) calculations] we derive 95%-C.L. limits on the neutrino mass difference δm^2 and mixing angle $\sin^2 2\theta$ for possible outcomes for the ^{37}Cl, ^{71}Ga, and Kamioka II experiments and the assumption of two-flavor oscillations. We find that ^{71}Ga counting rates as large as 128 solar-neutrino units (SNU) or as small as 4 SNU are not ruled out by present 95%-C.L. results from the ^{37}Cl and Kamioka II experiments, given possible solar and nuclear cross-section uncertainties. Considering all three of the experiments, ^{37}Cl (existing results), Kamioka II (existing results), and ^{71}Ga (hypothesized results), we find the allowed neutrino parameters form two distinct "islands" in the δm^2-$\sin^2 2\theta$ plane for ^{71}Ga results between 20 and 100 SNU, even with our restrictive assumption of oscillations between only two flavors. Thus additional experiments may be required to distinguish between solutions that are each consistent with the results from the ^{37}Cl, ^{71}Ga, and Kamioka II experiments. We explore the implications of future Kamioka II results of improved accuracy. To permit analyses of new experiments that focus on individual fluxes, we also present separate predictions of the MSW effect for ^{7}Be and ^{3}He$+p$ (hep) neutrinos.

I. INTRODUCTION

Mikheyev and Smirnov[1] pointed out that flavor oscillations of solar neutrinos could be greatly enhanced in matter. Their mechanism depends on an effective density-dependent contribution to the electron-neutrino mass arising from charged-current scattering off solar electrons, a phenomenon first discussed by Wolfenstein.[2] As large reductions in the neutrino flux occur for small vacuum mixing angles, the Mikheyev-Smirnov-Wolfenstein (MSW) mechanism offers a plausible particle-physics solution to the ^{37}Cl solar-neutrino puzzle. It is also now clear that solar-neutrino experiments provide a unique opportunity to study neutrino mass differences in the range of 10^{-2} to 10^{-4} eV.

The ν_e flux reduction caused by the MSW mechanism is energy dependent: By adjusting the particle-physics parameters, one can preferentially suppress the flux of high-, low-, or intermediate-energy neutrinos in the solar spectrum. Uncertainties in the standard solar model can also affect the relative numbers of high-energy (^{8}B) and low-energy (*pp*, *pep*, ^{7}Be,...) neutrinos. As a result, there is a subtle interplay between solar-model uncertainties and the particle physics governing neutrino oscillations. Indeed, though the production of iso-SNU (solar-neutrino-unit) curves for various experiments is now a minor industry, previous studies have either not included the uncertainties from the standard solar model or have included them by assuming their effects were independent of the MSW solution considered. (An example of the latter is given by Ref. 3, where the need for an analysis like the present was noted.) However, the energy depen-

dence of the MSW effect (which leads to different reductions and spectrum distortions for each neutrino source) can be correctly folded with solar-model flux uncertainties by Monte Carlo calculations in which the solar input parameters are varied according to their estimated probability distributions. The changes induced in the fluxes from neutrino-producing reactions are strongly correlated because variations in physical parameters (e.g., the solar temperature or nuclear reaction rates) affect all reactions. A correct Monte Carlo treatment of the uncertainties in solar parameters includes these correlations. Experimentalists are familiar with Monte Carlo uncertainty estimates in complicated experiments where various effects are coupled; a complicated system such as the standard solar model poses similar difficulties for the theoretician.

The intent of this paper is to account for solar-model uncertainties in determining quantitative constraints on the vacuum mixing angle $\sin^2 2\theta$ and mass difference $\delta m^2 = m_1^2 - m_2^2$, given possible outcomes for the ^{37}Cl, ^{71}Ga, and Kamioka II experiments and the assumption of two-flavor oscillations. We present, in a series of graphs, the 95%-C.L. standard solar-model constraints on $\sin^2 2\theta$ and δm^2 for these experiments. The calculations were performed by combining a fast but accurate analytical treatment of MSW oscillations with the flux predictions of a set of 1000 standard solar models that were generated by a proper Monte Carlo treatment of uncertainties in solar parameters.

Our approach allows us to derive limits on δm^2 and $\sin^2 2\theta$ given multiple experimental constraints. These limits can be more restrictive than those that would be obtained from the simple intersections of the 95%-C.L. curves for the respective experiments. In the case of ^{71}Ga, we find that nuclear and solar-model uncertainties combine to permit counting rates as large as 128 SNU and as small as 4 SNU, given present results from the ^{37}Cl and Kamioka II experiments. We also find, for a broad range of possible ^{71}Ga outcomes, that two distinct MSW solutions arise, corresponding to separated regions in the δm^2-$\sin^2 2\theta$ plane. Preliminary results from the Kamioka II experiment provide weak constraints on neutrino parameters. We discuss the important new constraints that can be derived from future Kamioka II results of improved accuracy. We also present separate predictions of the MSW effect for ^{7}Be and ^{3}He$+p$ (hep) neutrinos; these results will be useful in designing and analyzing new experiments that focus on these neutrino sources.

II. TREATMENT OF THE MSW MECHANISM

Although the differential equations governing neutrino propagation in the Sun can be integrated numerically, this approach is not feasible given the scale of the calculations needed here: for each point on a dense grid in the $\sin^2 2\theta$-δm^2 plane (121×81 was chosen), calculations were performed for about 240 neutrino energies spanning the solar spectrum. As the finite extent of the neutrino-producing core was treated carefully, about 130 integrations were needed for each energy. Thus a total of 3×10^8 separate MSW calculations are required.

Oscillation probabilities were calculated with the finite Landau-Zener (FLZ) approximation, an accurate analytic result derived by one of us.[3] This approximation is obtained by replacing the solar density in the narrow resonance region by a linear function having the correct magnitude and first derivative at the level-crossing point. Unlike the standard Landau-Zener approximation,[4] the integration is done only over the region bounded by the correct starting and ending solar densities. The resulting probability for detecting an electron neutrino a great distance from the Sun is

$$p_{\nu_e}(\infty) = \frac{\sin^2\theta}{2} + |a_e(t_s)|^2 \cos^2 2\theta - \sin 2\theta \cos 2\theta \, \mathrm{Re}[a_e(t_s) a_\mu(t_s)^*] , \quad (1)$$

where $a_e(t_s)$ and $a_\mu(t_s)$, the electron and muon neutrino amplitudes at the solar surface, can be written in terms of parabolic cylinder functions. The explicit expressions are given in Ref. 3. The FLZ approximation properly reduces to the standard Landau-Zener form[4] in the limit in which the neutrino is produced and observed at points sufficiently distant from the resonance region that its propagation is entirely adiabatic at these points. The FLZ approximation also contains the adiabatic approximation in the appropriate limit, and remains accurate for large mixing angles and within the resonance (nonadiabatic) region, where one or both of the simpler approximations (adiabatic or standard Landau-Zener) may fail. For mixing angles $\sin^2 2\theta \lesssim 0.1$, the FLZ approximation is virtually exact. Detailed comparisons with "exact" numerical results for large mixing angles ($\sin^2 2\theta = 0.5$) showed a maximum error in $p_{\nu_e}(\infty)$ of approximately 0.02 (Ref. 3).

The FLZ approximation requires evaluation of parabolic cylinder functions of complex argument and index. An efficient and accurate numerical algorithm can be obtained by combining the power-series and asymptotic-series expansions, and by exploiting the reflection properties of these functions, as described in Ref. 3. It is the speed of this procedure that permitted us to undertake the present calculations.

No attempt was made in the present calculations to treat oscillations during transit of the Earth.[5] Terrestrial regeneration can appreciably affect large-mixing-angle results near $\delta m^2 \sim 10^{-6}$ eV^2. However plans are underway to separate day-night differences in the ^{37}Cl experiment, and clearly such separations are possible in direct counting experiments. Thus it may be best to estimate the terrestrial effects separately from the solar-oscillation effects treated here.

While the graphical results we present later in the paper will be adequate for most purposes, any reader requiring detailed oscillation probabilities can obtain the data files from the authors on request.

III. THE STANDARD SOLAR MODEL AND NEUTRINO FLUX UNCERTAINTIES

The current status of the standard solar model has been recently reanalyzed by Bahcall and Ulrich.[6] We are

interested here in the prediction of the individual neutrino fluxes, and the reasonable variations in these fluxes that can be achieved by changing the parameters of the standard solar model. In our calculations we include the five neutrino sources in the *pp* chain, the *pp* ($\epsilon_\nu \leq 0.420$ MeV, pep ($\epsilon = 1.442$ MeV), ^{7}Be [$\epsilon_\nu = 0.862$ MeV (89.7%), 0.384 MeV (10.3%)], ^{8}B($\epsilon_\nu \lesssim 15$ MeV), and ^{3}He+*p* (hep) neutrinos ($\epsilon_\nu \leq 18.77$ MeV), as well as the ^{13}N ($\epsilon_\nu \leq 1.199$ MeV) and ^{15}O ($\epsilon_\nu \leq 1.732$ MeV) neutrinos from the CNO cycle. The standard solar "best values"[5] for the fluxes are given in Table I. The β-decay sources produce neutrinos with an allowed spectrum (prior to oscillations) with the exception of the ^{8}B decay, where the final state in ^{8}Be* is a broad resonance. The ^{8}B neutrino spectrum was taken from the tabulated results of Ref. 7.

We treat the possible variations in these fluxes by considering the 1000 solar models of Ref. 6. These models were constructed by randomly varying five input parameters, the primordial heavy-element-to-hydrogen ratio Z/X and the cross section S factors for the *p*-*p*, ^{3}He-^{3}He, ^{3}He-^{4}He, and *p*-^{7}Be solar reactions, assuming normal distributions for each with the means and standard deviations of Ref. 6. These parameters are five of the dominant uncertainties in predicting the neutrino absorption rate for the ^{37}Cl experiment. Smaller uncertainties from radiative opacities, the solar luminosity, and the solar age were added using the specified uncertainties and partial derivatives of the fluxes with respect to solar-model parameters of Ref. 6. The validity of this procedure is demonstrated by the excellent agreement between detailed Monte Carlo simulations and the results obtained by flux partial derivatives (see, e.g., Fig. 9 of Ref. 6). The neutrino flux predictions of the 1000 models are the input to the calculations we describe later.

The spatial distributions of neutrino-producing sources within the Sun affect the MSW oscillations. The radial distributions were taken from the tabulated results of Ref. 6 (see Tables 9 and 10 of this reference). These distributions do not change appreciably with the solar parameter variations described above, and thus were held fixed in our calculations.

TABLE I. Summary of neutrino-producing reactions of the *pp* chain and CNO cycle and the corresponding standard-model fluxes at the Earth's surface.

Source	$E_\nu^{\max}$ (MeV)	Flux (10^{10}/cm^{2}s)[a]
$p+p \rightarrow {}^2\mathrm{H}+e^+ +\nu$	0.42	6.0
$^{13}\mathrm{N} \rightarrow {}^{13}\mathrm{C}+e^+ +\nu$	1.20	6.1×10^{-2}
$^{15}\mathrm{O} \rightarrow {}^{15}\mathrm{N}+e^+ +\nu$	1.73	5.2×10^{-2}
$^8\mathrm{B} \rightarrow {}^8\mathrm{Be}+e^+ +\nu$	14.06[b]	5.8×10^{-4}
$^3\mathrm{He}+p \rightarrow {}^4\mathrm{He}+e^+ +\nu$	18.77	7.6×10^{-7}
$^7\mathrm{Be}+e^- \rightarrow {}^7\mathrm{Li}+\nu$	0.86 (90%)	0.47
	0.38 (10%)	
$p+e^- +p \rightarrow {}^2\mathrm{H}+\nu$	1.44	1.4×10^{-2}

[a]From Ref. 6.

[b]Value for the center of the ^{8}Be broad resonance populated in the decay of ^{8}B. See Ref. 7.

IV. NEUTRINO ABSORPTION CROSS SECTIONS

The range of responses for the ^{37}Cl (Ref. 8), ^{71}Ga (Ref. 9), and Kamioka II (Ref. 10) detectors depends not only on the values of the neutrino fluxes, but also on the detector cross sections. To assess the associated nuclear-

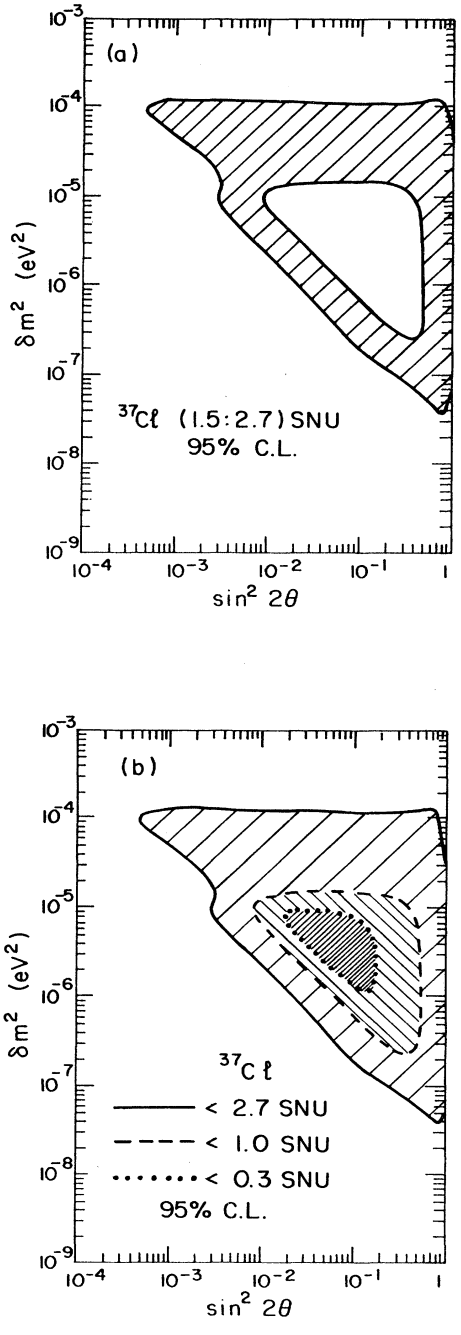

FIG. 1. (a) The unshaded regions show those values of δm^2 and $\sin^2 2\theta$ that are excluded at 95% C.L. by the ^{37}Cl counting rate of 2.1±0.6 SNU, given known uncertainties in the standard solar model. The corresponding results for hypothetical upper bounds of 2.7, 1.0, and 0.3 SNU are shown in (b).

physics uncertainties, we consider the effects of varying the cross section between reasonable minimum and maximum values.

The ^{37}Cl neutrino absorption cross sections for transitions to states below 6.02 MeV in ^{37}Ar can be determined[11] from the ^{37}Ar lifetime and the measured delayed proton spectrum following the β decay of the mirror nucleus ^{37}Ca, assuming isospin invariance. We adopt the relative log(ft) values of Sextro, Gough, and Cerny.[12] The normalization can be fixed by the log(ft) value for the analog transition, which could reasonably range between 3.26 and 3.30, depending on the Gamow-Teller contribution. These choices determine the maximum and minimum cross sections, respectively, for states below 6.02 MeV. In addition, (p,n) measurements show a strong Gamow-Teller peak [B(GT)$\sim$0.87] at an excitation energy of 7.65 MeV in ^{37}Ar (Ref. 13). As discussed in Ref. 14, the procedures followed by Sextro, Gough, and Cerny in analyzing the ^{37}Ca delayed proton spectrum would count this strength at a fraction of its true value while shifting it to lower energies. Therefore we omit the 7.65-MeV complex in estimating the minimum ^{37}Cl cross

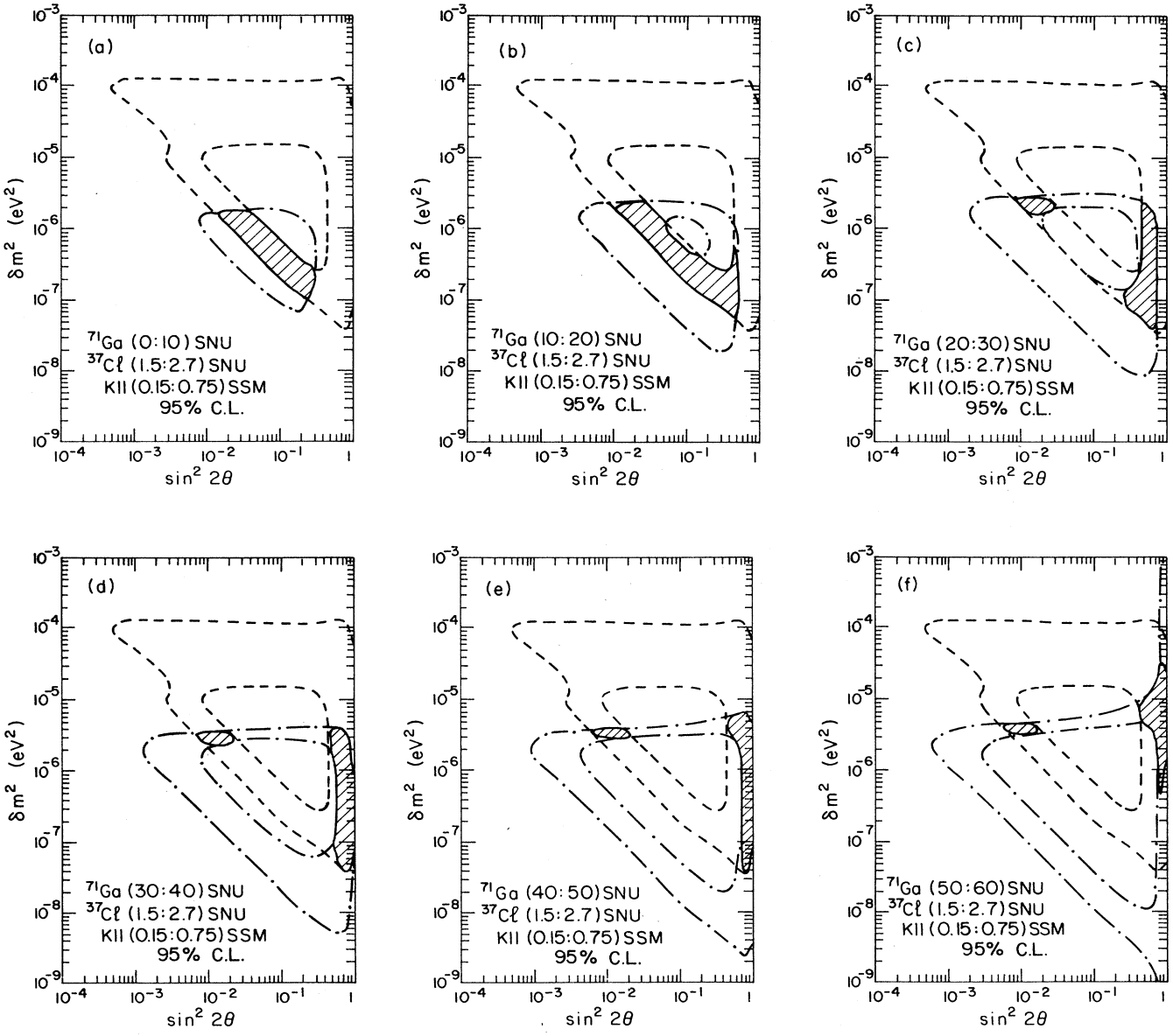

FIG. 2. The unshaded regions are excluded at 95% C.L. by combining the ^{37}Cl result (and preliminary Kamioka II result) with potential ^{71}Ga results. The 95% C.L. boundaries imposed separately by the ^{37}Cl and ^{71}Ga experiments are given by the dashed and dotted-dashed contours, respectively. Note that the shaded (allowed) regions cannot be obtained from the simple intersection of the regions enclosed by the dashed and dotted-dashed contours. Also note the considerable overlap of the shaded regions in successive graphs.

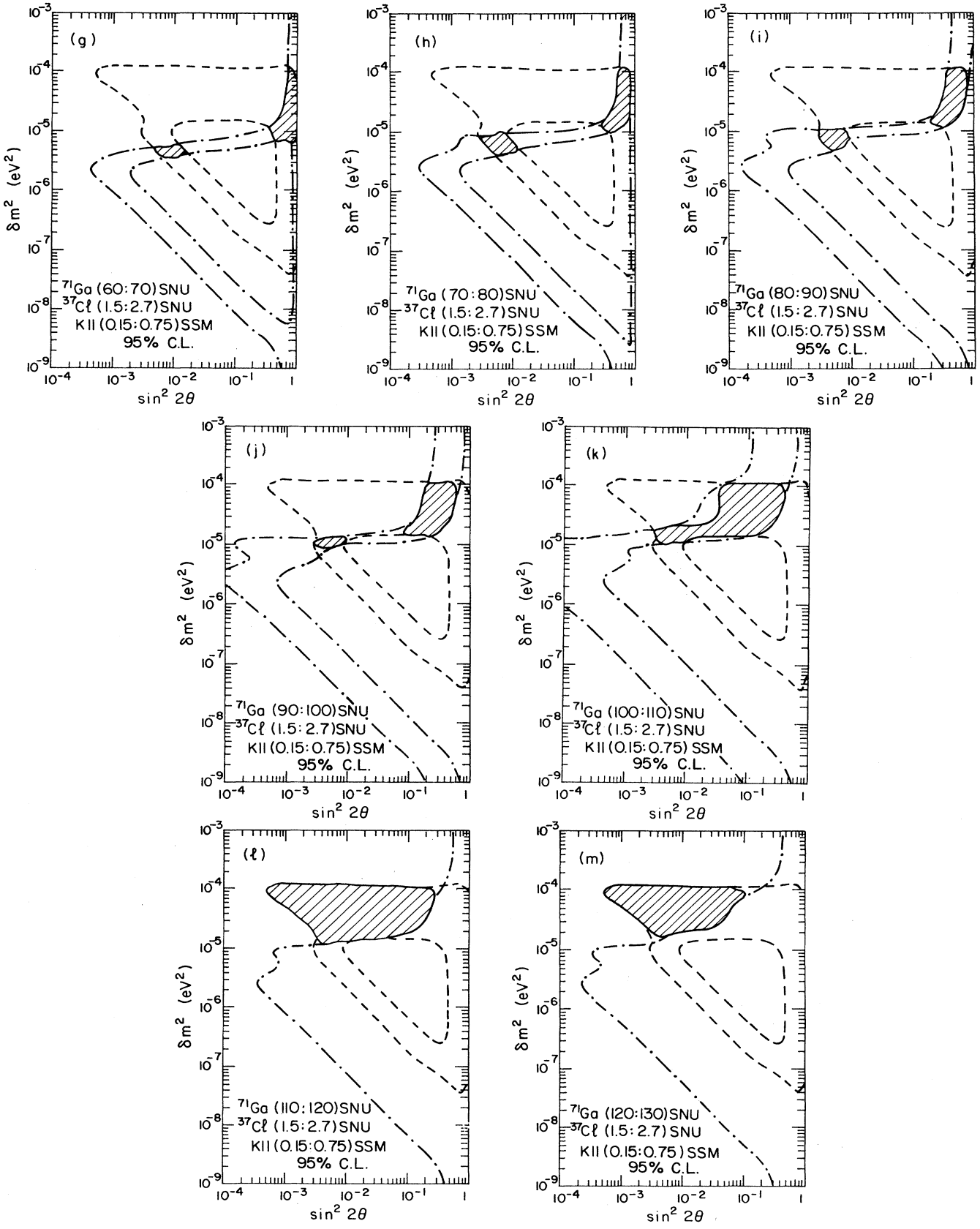

FIG. 2. (*Continued*).

section, while including it at full strength in the maximum.

For the ^{71}Ga detector, the strength of the transition to the ground state of ^{71}Ge is known accurately from the ^{71}Ge β decay rate. The (p,n) measurements of Krofcheck[15] provide the B(GT) profile for other ^{71}Ge bound states. Comparisons of forward-angle (p,n) B(GT) mappings with known β-decay strengths in light nuclei generally support the reliability of this technique at the level of $\pm 10\%$ (Ref. 16). Unfortunately few tests have been made for medium and heavy nuclei. Pending such tests, we adopt a generous estimate of the possible error in the derived ^{71}Ge B(GT) profile of a factor of 2 (following the procedure of Ref. 6). That is, we scale Krofcheck's B(GT) values by 0.5 to obtain our estimated minimum cross section, and by 2 to obtain the maximum.

The (ν_e,e) elastic scattering cross section for the Kamioka II detector is very well known. We adopt an uncertainty of $\pm 5\%$. The counting rate also depends on the efficiency for recording scattered electrons. The detector records electron events and an associated apparent energy ϵ_A of the event, determined by the number of phototubes triggered. Given an electron of energy ϵ_T, the probability of a recorded event is[17]

$$P(\epsilon_T)=\int_{\epsilon_A^{\min}}^{\epsilon_A^{\max}} d\epsilon_A f(\epsilon_A) p(\epsilon_A,\epsilon_T) , \tag{2}$$

where $p(\epsilon_A,\epsilon_T)$ is the probability that a recorded event of apparent energy ϵ_A came from an electron of true energy ϵ_T, and $f(\epsilon_A)$ is the detector efficiency for events of apparent energy ϵ_A. The efficiency function

$$f(\epsilon_A)=\begin{cases} 1-\exp\{-[(\epsilon_A-\epsilon_T)/4]^{2.03}\}, & \epsilon_A>\epsilon_T , \\ 0 \quad \text{otherwise} , \end{cases} \tag{3}$$

where ϵ_A is measured in MeV and $\epsilon_T=4.2$ MeV, is an accurate analytic approximation to measured results.[18,19] The Kamioka II resolution is approximately Gaussian:[18,19]

$$p(\epsilon_T,\epsilon_A)=k\exp[-(\epsilon_A-\epsilon_T)^2/2\sigma(\epsilon_A)^2] ,$$
$$\sigma(\epsilon_A)=0.22\epsilon_A\left[\frac{10\text{ MeV}}{\epsilon_A}\right]^{1/2} . \tag{4}$$

The normalization k is fixed by the condition $\int_{m_e}^{\infty} d\epsilon_A p(\epsilon_T,\epsilon_A)=1$. Note, however, that the integration in Eq. (1) is restricted by $\epsilon_A^{\min}$ and $\epsilon_A^{\max}$, software cuts made in the Kamioka II (KII) experiment to reduce background events. The experimenters currently use $\epsilon_A^{\min}=9.3$ MeV and $\epsilon_A^{\max}=15$ MeV (Ref. 21). As lower values of $\epsilon_A^{\min}$ may be used in future analyses, we have also performed calculations for $\epsilon_A^{\min}=8$ MeV.

Throughout our Kamioka II calculations we assume that the oscillation occurs into a second flavor, rather than into some sterile species. Muon and tauon neutrinos also scatter off electrons via the neutral current, though with a cross section about $\frac{1}{6}$ that for electron neutrinos. Thus our calculated KII counting rates are sums of the electron and heavy-flavor contributions.

V. RESULTS

The counting rate in the ^{37}Cl experiment is 2.1 ± 0.6 SNU (95% C.L.) above known backgrounds.[8] Those values of δm^2 and $\sin^2 2\theta$ that could yield this result are shown by the shaded region in Fig. 1(a). The unshaded region is excluded with a confidence level of 95%: that is, at each point in the unshaded region fewer than 50 of our 1000 solar models yield a result of 2.1 ± 0.6 SNU. The allowed (shaded) region forms the familiar MSW triangle. Conversion of electron neutrinos to a second flavor will occur if there is a level crossing and if the neutrino propagation is adiabatic. We will refer to the horizontal band at larger δm^2 as the "level-crossing boundary" or "horizontal" solution: the adiabatic condition is satisfied, but only higher-energy solar neutrinos experience a level crossing and are converted to a different flavor. The lower-energy neutrinos do not and thus contribute at nearly full strength to the ^{37}Cl experiment. The "diagonal" or "adiabatic boundary" band runs to much smaller δm^2. For these smaller δm^2 a level crossing will occur. However at the level crossing the transition for higher-energy neutrinos is highly nonadiabatic, so these neutrinos are not converted to a different flavor and would be counted in the ^{37}Cl experiment. The propagation of the lower-energy neutrinos is approximately adiabatic, so these neutrinos are converted. The "large mixing angle" or "vertical" band corresponds to the region where much of the flux reduction is attributable to vacuum oscillations. Thus the entire neutrino spectrum is partially converted. Of course, near the vertices of the triangle hybrid solutions appear: the structure appearing

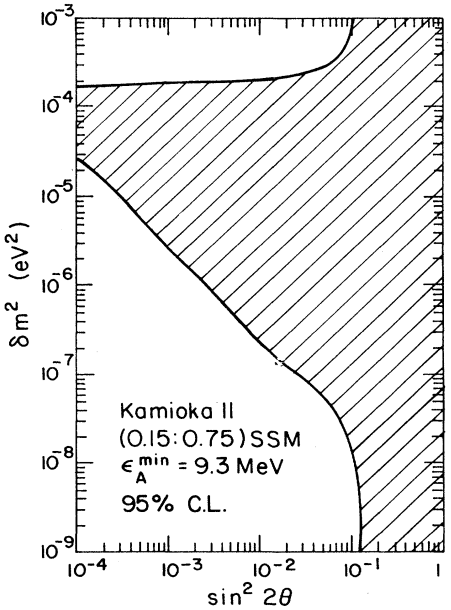

FIG. 3. The unshaded region is excluded at 95% C.L. by the preliminary Kamioka II result, 0.45 ± 0.30 of the best-value standard-model counting rate.

near the small-angle vertex is the result of a simultaneous breakdown in the adiabatic and level-crossing conditions for the high- and low-energy neutrinos, respectively.

The ^{37}Cl counting rate is derived from events above known backgrounds. One cannot exclude the possibility that some, or even most, of these events may originate from unknown backgrounds, i.e., sources other than solar neutrinos. Figure 1(b) takes this possibility into account by providing contours for different assumed limits on the rate of solar-neutrino events. The regions outside solid, dashed, and dotted contours would be excluded (95% C.L.) given upper bounds on the ^{37}Cl counting rate of 2.7, 1.0, and 0.3 SNU, respectively. These results will be of special interest if additional (nonsolar) backgrounds are identified in the ^{37}Cl experiment.

In Fig. 2 we combine possible outcomes of the ^{71}Ga experiment with the existing constraints from the ^{37}Cl and Kamioka II experiments.[20] (Kamioka II, which we discuss below, presently imposes only weak constraints at 95% C.L. The results of Fig. 2 are virtually unchanged by the omission of the Kamioka II data.) The regions within the dashed and dashed-dotted curves are the al-

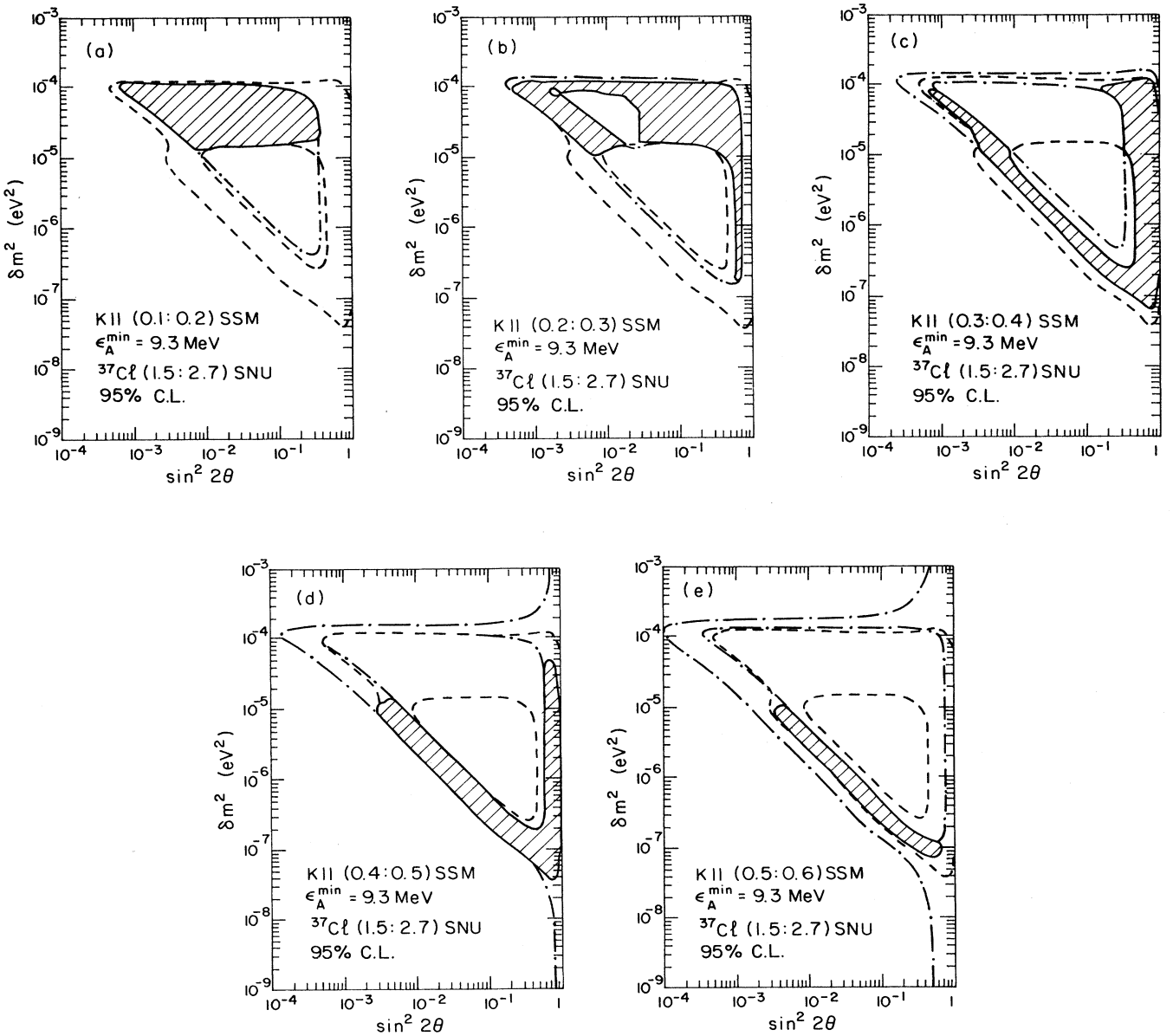

FIG. 4. The unshaded regions are excluded at 95% C.L. by combining the ^{37}Cl result with potential outcomes of the Kamioka II experiment. The 95% C.L. boundaries imposed separately by the ^{37}Cl and Kamioka II experiments are given by the dashed and dotted-dashed contours. Fractional Kamioka II rates above 0.6 are excluded by the ^{37}Cl result.

lowed regions for the separate ^{37}Cl and ^{71}Ga experiments, respectively. The unshaded regions are excluded at 95% C.L. when the ^{71}Ga and ^{37}Cl (and Kamioka II) results are combined. That is, the shaded areas define those regions of the δm^2-$\sin^2 2\theta$ plane where at least 50 of the solar models satisfy all three experimental constraints *simultaneously*. Thus the allowed (shaded) region is always smaller than (and contained within) the intersections obtained by overlaying the separate 95%-C.L. contours for ^{71}Ga and ^{37}Cl. A correct extraction of the constraints imposed by multiple experiments, including all the implicit solar-model correlations between neutrino fluxes from different nuclear reactions, is an important result of our Monte Carlo procedure.

No results are given for ^{71}Ga counting rates above 130 SNU: the maximum rate consistent with the ^{37}Cl result is 128 SNU. A counting rate $\sim$128 SNU that is consistent with the ^{37}Cl experiment may seem surprising, as this is close to the best-estimate value of 132 SNU for the ^{71}Ga counting rate in the absence of oscillations. However, the large uncertainty we have adopted for the ^{71}Ge excited-state contribution to the ^{71}Ga cross section combines with solar-model uncertainties to yield this result.

The shaded region for small ^{71}Ga counting rates ($\leq$20 SNU) is connected and lies within the ^{37}Cl "diagonal" solution. For counting rates between 20 and 100 SNU, the allowed region forms two topologically distinct "islands:" one within the "vertical" ^{37}Cl solution and the other within the "diagonal" solution. Thus the combined results of the ^{71}Ga, ^{37}Cl, and Kamioka II experiments lead to multiple neutrino solutions even for our restrictive assumptions of two-flavor oscillations and standard solar-model physics. These islands move apart (in $\sin^2 2\theta$) and toward larger δm^2 as the assumed ^{71}Ga counting rate increases from 20 to 100 SNU. For counting rates between 100 and 130 SNU, a single region within the "horizontal" ^{37}Cl solution is allowed.

There exists a preliminary result from the Kamioka II experiment of a counting rate, as a fraction of the ^{8}B flux best-estimate result in the absence of oscillations, of 0.46 ± 0.13(stat.)±0.08(syst.) (1σ) (Ref. 20). This limit was derived for the choice $\epsilon_A^{\min}=9.3$ MeV, for which the standard-model best-value counting rate in the absence of oscillations is 0.017 SNU (per target electron). We doubled the statistical error (0.46 ± 0.26(stat.)±0.08(syst.)) to approximate a 95%-C.L. result. The lower bound is of no significance for oscillations between two flavors: the maximum theoretical reduction in the counting rate is approximately a factor of 6. The Kamioka II 95%-C.L. upper bound is already of importance, excluding the unshaded region of Fig. 3 corresponding to regions of the δm^2-$\sin^2 2\theta$ plane where oscillation effects on solar neutrinos are quite small. Note, however, that these regions are independently excluded by the ^{37}Cl result (although there is no direct experimental proof that the ^{37}Cl events are of solar origin, in contrast with KII).

The Kamioka II experiment and future water Cherenkov detectors will ultimately produce improved constraints. The importance of this is illustrated by Fig. 4, where the unshaded regions are excluded at 95% C.L. given the ^{37}Cl result and various assumed counting rate limits from Kamioka II. The dashed and dotted-dashed contours give the separate ^{37}Cl and assumed Kamioka II constraints, respectively, similar to Fig. 2. Note that fractional Kamioka II counting rates above 0.6 are excluded by the ^{37}Cl experiment. Counting rates above 0.5 are only compatible with portions of the "diagonal" solu-

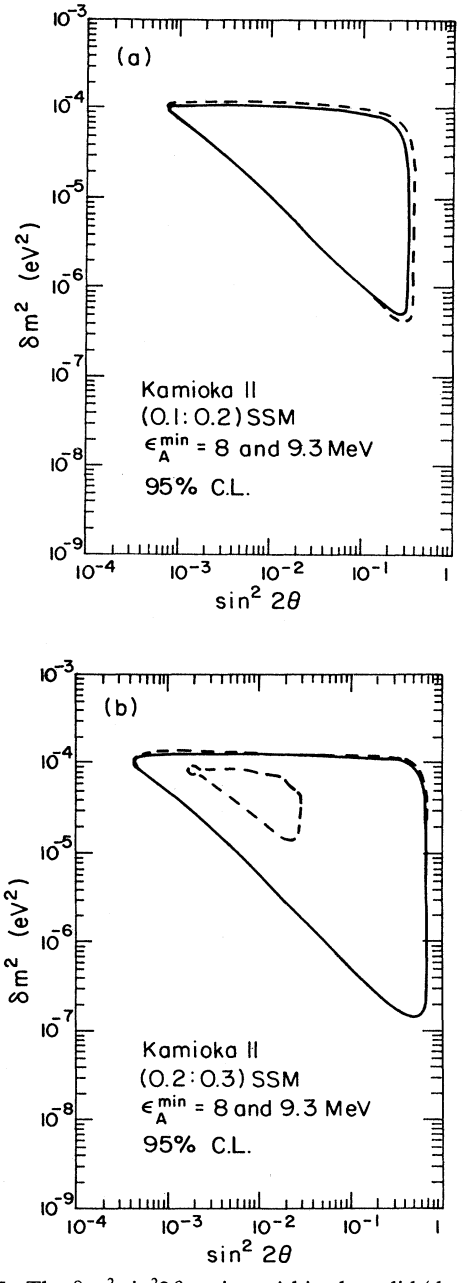

FIG. 5. The δm^2-$\sin^2 2\theta$ region within the solid (dashed) contours is allowed given the indicated Kamioka II fractional counting rate for $\epsilon_A^{\min}=8$ MeV (9.3 MeV). The "hole" in (b) is the principal exception to the general rule that the 8 and 9.3 MeV contours are difficult to distinguish.

tion, while those between 0.3 and 0.5 are compatible with regions within the "diagonal" or "vertical" solutions. Below 0.3 only the "horizontal" solution and a narrow strip within the "vertical" solution are allowed.

If backgrounds permit, future analyses of the Kamioka II data may employ lower values for $\epsilon_A^{\min}$ in order to include more solar-neutrino events. The choice $\epsilon_A^{\min}=8$ MeV yields a best-value standard-model counting rate of 0.028 SNU in the absence of oscillations, in contrast with the 0.017-SNU 9.3-MeV result. Thus a lower threshold will permit the experimentalists to obtain a more precise result. However, as the results in Fig. 4 is presented as a fraction of the best value, they vary only slowly with $\epsilon_A^{\min}$. We performed a full set of $\epsilon_A^{\min}=8$ MeV calculations and found differences that could be easily distinguished only for fractional counting rates below 0.3. The two largest differences are shown in Fig. 5. The small hole that appears in Fig. 5(b) for $\epsilon_A^{\min}=9.3$ MeV disappears at 8 MeV: when a broader range of neutrino energies is accepted, the oscillation effects are slightly less pronounced.

In Fig. 6 we give analogous results for the hypothetical case where the ^{8}B flux is turned off, so that only the high-energy hep neutrinos remain. In these calculations we used the Kamioka II efficiency and resolution functions described earlier, but adopted $\epsilon_A^{\min}=13.5$ MeV in Eq. (2). Thus we are sampling the high-energy end of the hep spectrum, or those neutrinos that could in principle be distinguished from ^{8}B neutrinos. (To do this experimentally, however, may require better resolution than presently possible in Kamioka II: the "spill-over" of lower-energy ^{8}B events whose apparent energy is higher could obscure the hep signal in the present detector.) As expected, Fig. 6 is similar to the dashed-dotted curves of Fig. 4, apart from a shift to larger δm^2. While the hep

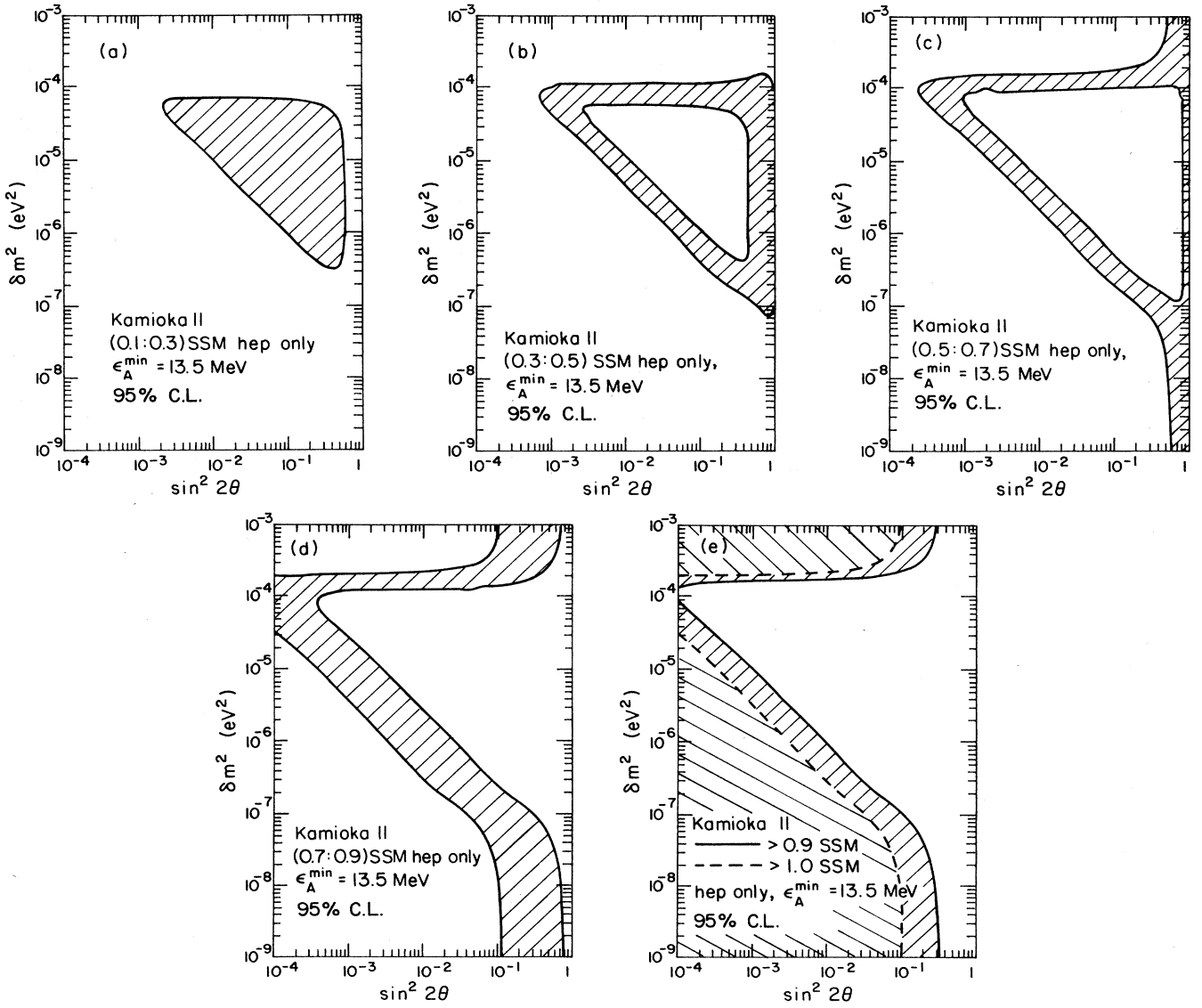

FIG. 6. Results for the hypothetical case where the ^{8}B flux is removed, leaving only hep neutrinos to contribute to the Kamioka II experiment. See the text for a discussion of the threshold cut $\epsilon_A^{\min}$. The unshaded regions are excluded at 95% C.L.

flux is not very sensitive to solar-model uncertainties, the nuclear cross section for the ^3He+p reaction is poorly known.[5,17] However, this uncertainty is an overall scale factor that does not affect results quoted as a fraction of the best-value standard solar-model rate.

Finally, in Fig. 7 we give results for a hypothetical detector capable of recording the higher energy (862 keV) branch of the ^7Be neutrinos. Several contemplated detectors may be able to isolate the flux.

VI. DISCUSSION AND SUMMARY

How is the present discussion different from previous discussions of matter-enhanced neutrino oscillations? First, our Monte Carlo approach takes into account the complicated correlations between different neutrino flux sources in the standard solar model, and properly folds these with the energy-dependent MSW flux reductions and nuclear response functions (including the associated nuclear cross-section uncertainties). Second, our prescription is easily generalized to provide confidence-level contours in the δm^2-$\sin^2 2\theta$ plane for combinations of two or more experimental constraints. The calculations are not numerically trivial: even with the restrictive assumption of two-flavor oscillations, approximately 3×10^8 separate MSW solutions are needed to adequately cover the required ranges of neutrino parameters and energies, and to account for the spatial extent of the neutrino-producing portion of the solar core. The calculations are feasible because we exploit the accurate FLZ approximation, which expresses the MSW oscillation probability in terms of parabolic cylinder functions.

Even within the restrictive theoretical framework of two-flavor oscillations and standard solar-model physics, we find that the existing and in-progress solar-neutrino experiments may be insufficient to determine uniquely the

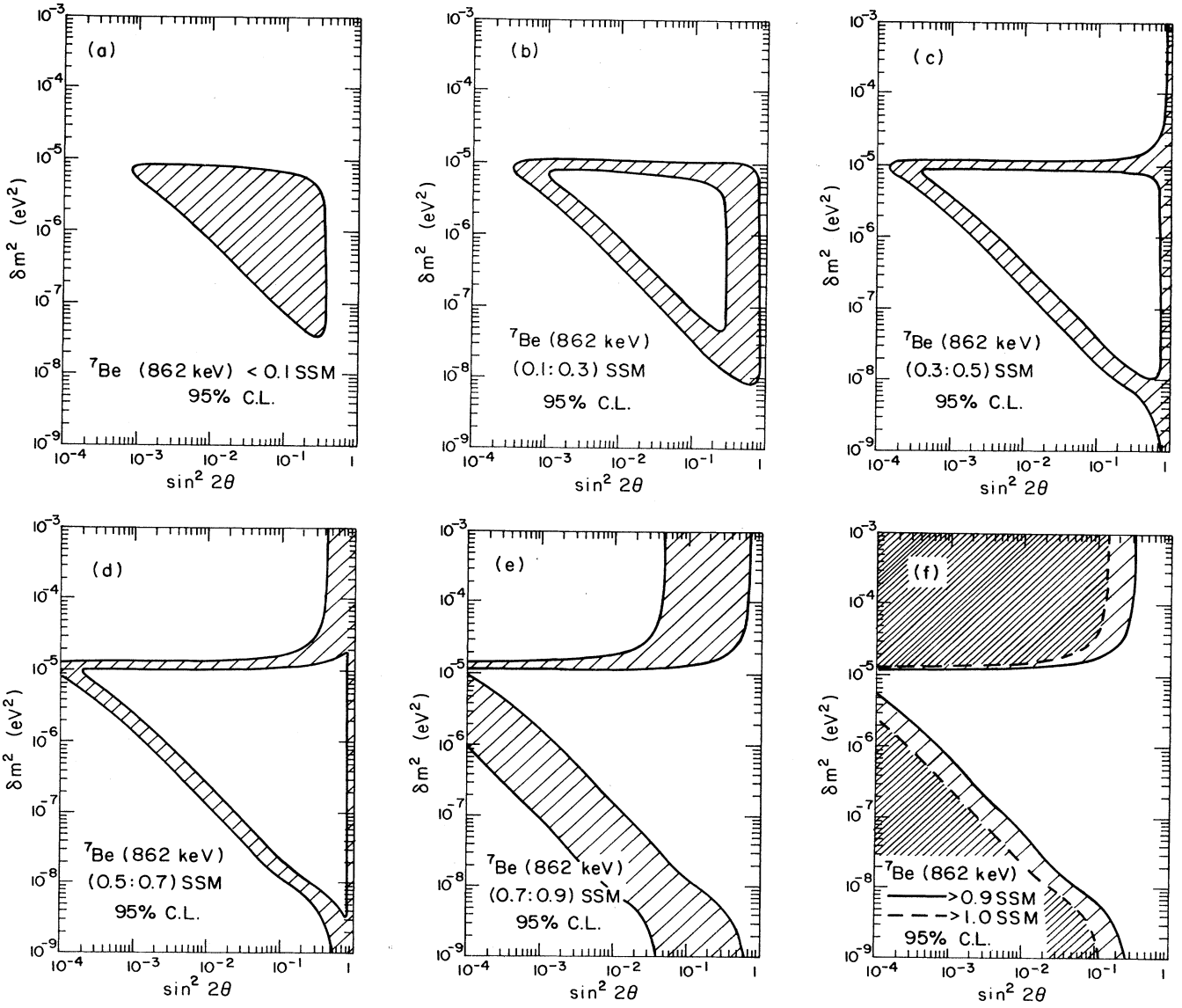

FIG. 7. As in Fig. 6, only for a hypothetical detector capable of detecting the high-energy (862-keV) branch of the ^7Be neutrino flux.

set of permitted neutrino parameters. For ^{71}Ga counting rates between 20 and 100 SNU, the solutions form two separated "islands" in the δm^2-$\sin^2 2\theta$ plane. If the ^{71}Ga counting rate is found to lie in this range, new experiments would be required to distinguish between the two solutions.

Given the existing results from the ^{37}Cl and Kamioka II experiments, we find that ^{71}Ga rates as large as 128 SNU and as small as 4 SNU are not ruled out at the 95% C.L. These results can be compared to the best standard model value of 132 SNU. This extended range would be narrower if the ^{8}B and ^{7}Be neutrino absorption cross sections for ^{71}Ga were known more reliably. The constraints provided by the existing limits from the Kamioka II experiment are rather weak and are illustrated in Fig. 3. Future results from Kamioka II or other neutrino-electron scattering experiments are potentially more restrictive, as shown in Figs. 4 and 5.

What new fluxes need to be studied experimentally? The hep neutrinos and ^{7}Be neutrinos can tell us a great deal about both the standard solar model and possible matter-enhanced neutrino oscillations (see the discussion in Ref. 17): The former is a high-energy but relatively solar model-independent neutrino flux, while the latter is a low-energy but solar-model-dependent flux. Thus these fluxes respond differently from the ^{8}B or *pp* neutrinos to changes in neutrino and solar-model parameters. Figures 6 and 7 show the constraints that could be obtained from experiments sensitive to these fluxes.

ACKNOWLEDGMENTS

This work was supported in part by the U.S. Department of Energy and the National Science Foundation.

[1]S. P. Mikheyev and A. Yu. Smirnov, Yad. Fiz. **42**, 1441 (1985) [Sov. J. Nucl. Phys. **42**, 913 (1985)]; Nuovo Cimento **9C**, 17 (1986); in *'86 Massive Neutrinos in Astrophysics and Particle Physics,* proceedings of the XXIth Rencontre de Moriond (VI Moriond Workshop), Tignes, France, 1986, edited by O. Fackler and J. Tran Thanh Van (Editions Frontières, Gif-sur-Yvette, 1986), p. 355; H. Bethe, Phys. Rev. Lett. **56**, 1305 (1986); S. P. Rosen and J. M. Gelb, Phys. Rev. D **34**, 969 (1986).

[2]L. Wolfenstein, Phys. Rev. D **17**, 2369 (1978); **20**, 2634 (1979).

[3]W. C. Haxton, Phys. Rev. D **35**, 2352 (1987).

[4]W. C. Haxton, Phys. Rev. Lett. **57**, 1271 (1986); S. J. Parke, *ibid.* **57**, 1275 (1986); L. D. Landau, Phys. Z. Sowjetunion **2**, 46 (1932); C. Zener, Proc. R. Soc. London **A137**, 696 (1932); E. C. G. Stueckelberg, Helv. Phys. Acta **5**, 369 (1932).

[5]M. Cribier, W. Hampel, J. Rich, and D. Vignaud, Phys. Lett. B **182**, 89 (1986); A. J. Baltz and J. Weneser, Phys. Rev. D **35**, 528 (1987).

[6]J. N. Bahcall and R. K. Ulrich, Rev. Mod. Phys. **60**, 297 (1988).

[7]J. N. Bahcall and B. R. Holstein, Phys. Rev. C **33**, 2121 (1986).

[8]R. Davis, Jr., in *Seventh Workshop on Grand Unification,* proceedings, ICOBAN '86, Toyama, Japan, 1986, edited by J. Arafune (World Scientic, Singapore, 1987), p. 237; J. K. Rowley, B. T. Cleveland, and R. Davis, Jr., in *Solar Neutrinos and Neutrino Astronomy,* edited by M. L. Cherry, W. A. Fowler, and K. Lande (AIP Conf. Proc. No. 126) (AIP, New York, 1985), p. 1.

[9]T. Kirsten, in *'86 Massive Neutrinos in Astrophysics and Particle Physics* (Ref. 1), p. 119; I. R. Barabanov, in *Solar Neutrinos and Neutrino Astronomy* (Ref. 8), p. 175.

[10]E. W. Beier, in *Seventh Workshop on Grand Unification* (Ref. 8), p. 79; K. S. Hirata *et al.*, Phys. Rev. D **38**, 448 (1988); K. S. Hirata *et al.*, Phys. Rev. Lett. **61**, 2653 (1988).

[11]J. N. Bahcall, Rev. Mod. Phys. **50**, 881 (1978).

[12]R. G. Sextro, R. A. Gough, and J. Cerny, Nucl. Phys. **A234**, 130 (1974).

[13]J. Rapaport *et al.*, Phys. Rev. Lett. **47**, 1518 (1981).

[14]E. G. Adelberger and W. C. Haxton, Phys. Rev. C **36**, 879 (1987).

[15]D. Krofcheck, Ph.D. thesis, Ohio State University, 1987; also see D. Krofcheck *et al.*, Phys. Rev. Lett. **55**, 1051 (1985).

[16]N. T. Taddeucci *et al.*, Nucl. Phys. **A469**, 125 (1988).

[17]J. N. Bahcall, *Neutrino Astrophysics* (Cambridge University Press, Cambridge, England, 1989), Secs. 13.1 and 13.2; J. N. Bahcall, J. M. Gelb, and S. P. Rosen, Phys. Rev. D **35**, 2976 (1987).

[18]M. Nakahata, Ph.D. thesis, Faculty of Sciences, University of Tokyo (Report No. UT-ICEPP-880-01).

[19]E. W. Beier (private communication).

[20]K. Hirata *et al.*, Phys. Rev. Lett. **63**, 16 (1989).